

PACS 77.80.Bh, 78.40.Ha

## **Dielectric permittivity of $(\text{Ag}_3\text{AsS}_3)_x(\text{As}_2\text{S}_3)_{1-x}$ superionic glasses and composites**

**I.P. Studenyak<sup>1</sup>, Yu.Yu. Neimet<sup>1</sup>, A.F. Orliukas<sup>2</sup>, A. Kežionis<sup>2</sup>, E. Kazakevičius<sup>2</sup>, T. Šalkus<sup>2</sup>**

<sup>1</sup>*Faculty of Physics, Uzhhorod National University,  
46, Pidhirna str., 88000 Uzhhorod, Ukraine*

<sup>2</sup>*Vilnius University, Faculty of Physics,  
9, Saulėtekio al., LT-10222 Vilnius, Lithuania  
E-mail: studenyak@dr.com*

**Abstract.** Complex dielectric permittivity of  $(\text{Ag}_3\text{AsS}_3)_x(\text{As}_2\text{S}_3)_{1-x}$  ( $x = 0.3-0.9$ ) superionic glasses and composites at 300 K were studied. A decrease of the real part of dielectric permittivity with frequency by almost five orders of magnitude as well as one dispersion region in glasses and two dispersion regions in composites, which is reflected in the dielectric loss spectra, were observed. Frequency dependences of dielectric permittivity within the range from 10 Hz to  $3 \times 10^9$  Hz were analyzed in the framework of the Cole-Cole model. Compositional behaviour of Cole-Cole parameters in  $(\text{Ag}_3\text{AsS}_3)_x(\text{As}_2\text{S}_3)_{1-x}$  ( $x = 0.3-0.9$ ) superionic glasses and composites was studied. The most substantial changes were observed with the transition from  $(\text{Ag}_3\text{AsS}_3)_{0.4}(\text{As}_2\text{S}_3)_{0.6}$  glass to  $(\text{Ag}_3\text{AsS}_3)_{0.5}(\text{As}_2\text{S}_3)_{0.5}$  composite and from  $(\text{Ag}_3\text{AsS}_3)_{0.6}(\text{As}_2\text{S}_3)_{0.4}$  composite to  $(\text{Ag}_3\text{AsS}_3)_{0.8}(\text{As}_2\text{S}_3)_{0.2}$  composite.

**Keywords:** superionic glasses, composites, dielectric permittivity, Cole-Cole parameters.

Manuscript received 31.01.14; revised version received 14.05.14; accepted for publication 12.06.14; published online 30.06.14.

### **1. Introduction**

Chalcogenide glasses, doped with metals, have attracted wide interest due to increased ionic conductivity. Such characteristic features of chalcogenide glasses as the presence of ion conduction pathways, phase separation, high mobility of conductive ions in the matrix of the chalcogenide glass make them applicable for creation of solid electrolyte batteries, electrochemical sensors, fuel cells, electrochromic displays, etc. [1]. It should be noted that in comparison with crystalline solid electrolytes, chalcogenide glasses are more technological, simple and lower-cost in production. The remarkable place among them is taken by the glasses of Ag-As-S ternary system

due to high values of electrical conductivity being mostly ionic [2].

Electrical conductivity of materials in the Ag-As-S system, prepared by different methods (doping of  $\text{As}_2\text{S}_3$  with Ag, silver dissolution), was studied by several researchers [2-10]. It was shown that the electrical conductivity of  $(\text{Ag}_2\text{S})_x(\text{As}_2\text{S}_3)_{1-x}$  glasses increases to display a step-like jump of nearly 5 orders of magnitude within the narrow concentration range  $9\% < x < 15\%$  [9]. At  $x < 5\%$  the electrical conductivity is typical for a semiconducting glass, while at  $x > 15\%$  it is representative of an ionic conductor. Interrelation between structural peculiarities and ionic transport were studied in Refs. [9, 10]. Recently, silver ion diffusion

was considered by S. Stehlik et al. using the random-walk model [11].

In Ref. [12], it was shown that after heating the  $(\text{Ag}_3\text{AsS}_3)_x(\text{As}_2\text{S}_3)_{1-x}$  ( $x = 0.3 - 0.6$ ) glasses and composites up to more than 450 K and subsequent cooling down to room temperature, formation of nanocrystals on the surface takes place, which leads to a sharp decrease of optical transparency. The temperature studies of optical absorption edge in  $(\text{Ag}_3\text{AsS}_3)_x(\text{As}_2\text{S}_3)_{1-x}$  glasses and composites were carried out in the work [13]. Besides, the frequency, temperature and compositional investigations of electrical conductivity in  $(\text{Ag}_3\text{AsS}_3)_x(\text{As}_2\text{S}_3)_{1-x}$  glasses and composites were performed in [14].

Now, it is of a great importance and actuality to obtain information concerning the dielectric response of the Ag-As-S system. Hence, the present study is focused on the investigation of the dielectric permittivity of  $(\text{Ag}_3\text{AsS}_3)_x(\text{As}_2\text{S}_3)_{1-x}$  ( $x = 0.3-0.9$ ) superionic glasses and composites in a wide frequency range from 10 Hz to 3 GHz at room temperature.

## 2. Experimental

Synthesis of vitreous compounds in the  $\text{Ag}_3\text{AsS}_3\text{-As}_2\text{S}_3$  system was carried out at temperatures 820-840 K with 24-h melt homogenization time from the corresponding components, which were synthesized beforehand from highly pure elemental substances. Glassy alloys were mixed periodically and subsequently cooled in the icy water (273 K). Six alloys in the concentration range of  $x = 0.3-0.9$  for  $(\text{Ag}_3\text{AsS}_3)_x(\text{As}_2\text{S}_3)_{1-x}$  superionic glasses and composites were chosen for the study. Measurements of complex dielectric permittivity were carried out within the range of frequencies 10 Hz–3 GHz at room temperature by a coaxial impedance spectrometer set-up [15].

## 3. Results

The frequency dependences of the real part of complex dielectric permittivity  $\epsilon'$  exhibit frequency dispersion and the low-frequency plateau corresponding to the limiting low-frequency bulk dielectric constant  $\epsilon_s$  should be reached (Fig. 1a). At still lower frequencies, the capacitance of the electrode, connected in series with the sample, causes a rapid increase of dielectric constant with decreasing frequency [16]. Composites  $(\text{Ag}_3\text{AsS}_3)_x(\text{As}_2\text{S}_3)_{1-x}$  with  $x = 0.5, 0.6$  and  $0.8, 0.9$  have two very distinct dispersion regions, which is well seen on the frequency dependence of dielectric loss  $\epsilon''$  (Fig. 1). With the frequency increase for the glasses and composites  $(\text{Ag}_3\text{AsS}_3)_x(\text{As}_2\text{S}_3)_{1-x}$  with  $x = 0.3-0.9$ , a decrease of  $\epsilon'$  by almost 5 orders of magnitude was revealed.

As one can see from Fig. 1b, the frequency dependences of the imaginary part of complex dielectric permittivity  $\epsilon''$  for  $(\text{Ag}_3\text{AsS}_3)_{0.3}(\text{As}_2\text{S}_3)_{0.7}$  and

$(\text{Ag}_3\text{AsS}_3)_{0.4}(\text{As}_2\text{S}_3)_{0.6}$  glasses display one maximum at the frequencies  $\nu = 120$  Hz and 337 Hz, respectively. With further addition of  $\text{Ag}_3\text{AsS}_3$  to the  $\text{As}_2\text{S}_3$  glassy matrix, the composites in  $\text{Ag}_3\text{AsS}_3\text{-As}_2\text{S}_3$  system are formed. In  $(\text{Ag}_3\text{AsS}_3)_{0.5}(\text{As}_2\text{S}_3)_{0.5}$  and  $(\text{Ag}_3\text{AsS}_3)_{0.6}(\text{As}_2\text{S}_3)_{0.4}$  composites, the maximum of the frequency dependence of  $\epsilon''$  moves stepwise to the higher frequency region and is observed at  $\nu = 6559$  Hz for  $(\text{Ag}_3\text{AsS}_3)_{0.5}(\text{As}_2\text{S}_3)_{0.5}$  and at  $\nu = 4956$  Hz for  $(\text{Ag}_3\text{AsS}_3)_{0.6}(\text{As}_2\text{S}_3)_{0.4}$  (Figs 1b and 2). Besides, for the above mentioned composites the additional peculiarities in a form of an asymmetry and a shoulder on the high-frequency wings of  $\epsilon''$  maxima are observed (see insert to Fig. 1b). It should be noted that for  $(\text{Ag}_3\text{AsS}_3)_{0.8}(\text{As}_2\text{S}_3)_{0.2}$  and  $(\text{Ag}_3\text{AsS}_3)_{0.9}(\text{As}_2\text{S}_3)_{0.1}$  two maxima are revealed on the frequency dependences of the imaginary part of complex dielectric permittivity. They are observed at  $\nu_1 = 139$  Hz and  $\nu_2 = 39244$  Hz for  $(\text{Ag}_3\text{AsS}_3)_{0.8}(\text{As}_2\text{S}_3)_{0.2}$  and at  $\nu_1 = 69$  Hz and  $\nu_2 = 59354$  Hz for  $(\text{Ag}_3\text{AsS}_3)_{0.9}(\text{As}_2\text{S}_3)_{0.1}$  at the frequency dependences of  $\epsilon''$  (Fig. 1b).

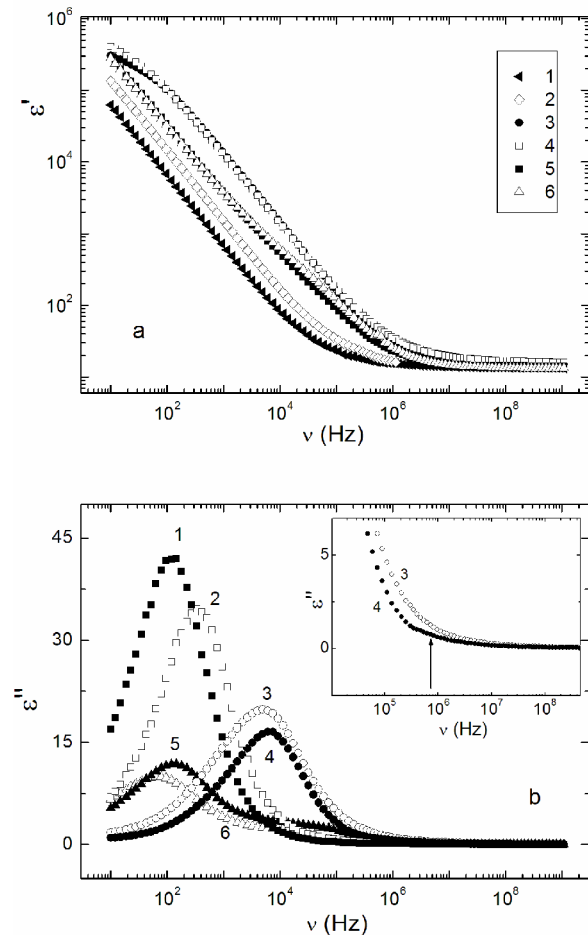


**Fig. 1.** Frequency dependences of the real  $\epsilon'$  (a) and imaginary  $\epsilon''$  (b) parts of the complex dielectric permittivity for various  $x = 0.3$  (1),  $0.4$  (2),  $0.5$  (3),  $0.6$  (4),  $0.8$  (5),  $0.9$  (6) in  $(\text{Ag}_3\text{AsS}_3)_x(\text{As}_2\text{S}_3)_{1-x}$  glasses and composites at  $T = 300$  K.

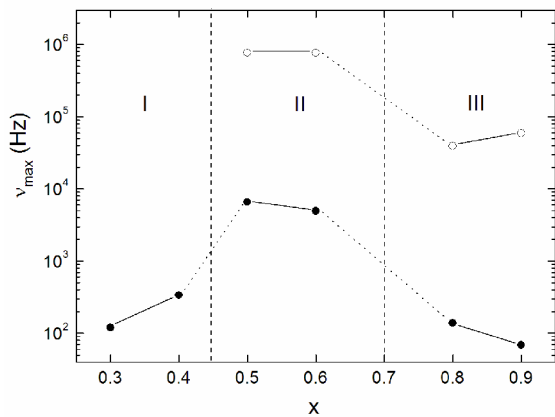


**Fig. 2.** Compositional dependences of maxima frequencies of the imaginary part of complex dielectric permittivity for  $(\text{Ag}_3\text{AsS}_3)_x(\text{As}_2\text{S}_3)_{1-x}$  glasses and composites at 300 K.

The obtained results on the dielectric permittivity are in a good agreement with the results of X-ray studies, which shows that the glasses of Ag–As–S system become separated after adding the proustite  $\text{Ag}_3\text{AsS}_3$  crystal to the base  $\text{As}_2\text{S}_3$  glass [14]. One can distinguish three different structural states in the whole compositional range of the  $\text{Ag}_3\text{AsS}_3$ – $\text{As}_2\text{S}_3$  system, namely: glassy state for  $x = 0$ – $0.4$  (I), composite state with crystalline smithite  $\text{AgAsS}_2$  inclusions for  $0.4 < x \leq 0.6$  (II), and a composite state with crystalline smithite  $\text{AgAsS}_2$  and proustite  $\text{Ag}_3\text{AsS}_3$  inclusions for  $0.6 < x < 1$  (III). Compositional changes of dielectric permittivity at the transitions from  $x = 0.4$  to  $0.5$  are related to the transition from the glassy structure at  $x \leq 0.4$  to the composite one with  $\text{AgAsS}_2$  crystalline inclusions at  $x \geq 0.5$ . Peculiarities of compositional behavior of dielectric permittivity at the transition from  $x = 0.6$  to  $0.8$  are due to the presence of crystalline  $\text{AgAsS}_2$  and  $\text{Ag}_3\text{AsS}_3$  inclusions in  $\text{As}_2\text{S}_3$  glassy matrix. Therefore, the compositional studies of dielectric permittivity in  $(\text{Ag}_3\text{AsS}_3)_x(\text{As}_2\text{S}_3)_{1-x}$  glasses and composites revealed the most significant changes occurring at the transitions

from  $x = 0.4$  to  $0.5$  and from  $x = 0.6$  to  $0.8$  (Figs 1 and 2). The above highlighted results were confirmed by the presence of the corresponding bands in the X-ray diffraction patterns of superionic  $(\text{Ag}_3\text{AsS}_3)_x(\text{As}_2\text{S}_3)_{1-x}$  glasses and composites [14].

#### 4. Discussion

For the advance analysis of the dielectric relaxation processes in  $(\text{Ag}_3\text{AsS}_3)_x(\text{As}_2\text{S}_3)_{1-x}$  glasses and composites, the well-known Cole-Cole equation was used [17]:

$$\varepsilon^*(\omega) = \varepsilon_\infty + \frac{(\varepsilon_s - \varepsilon_\infty)}{1 + (i\omega\tau_0)^{1-\alpha}},$$

where  $\varepsilon^* = \varepsilon' + i\varepsilon''$  is the complex dielectric permittivity ( $\varepsilon'$  is the dielectric constant and  $\varepsilon''$  – dielectric loss),  $\varepsilon_\infty$  – high frequency limiting value of dielectric permittivity  $\varepsilon'$  at  $\omega \rightarrow \infty$ ,  $\varepsilon_s$  – low frequency static dielectric permittivity at  $\omega \rightarrow 0$ ,  $\omega = 2\pi\nu$  – angular frequency ( $\nu$  – experimental frequency),  $\tau_0$  – most probabilistic mean relaxation time of the corresponding relaxation process (among all the relaxation times from the relaxation distribution function), and, finally,  $\alpha$  is a characteristic parameter (parameter of a width of the Cole-Cole relaxation distribution function) that assumes values between 0 and 1. The value  $\Delta\varepsilon = \varepsilon_s - \varepsilon_\infty$ , a finite change of the dielectric constant, is also known as a dielectric strength, or polarizability. It should be noted that  $\varepsilon_\infty$  is also a contribution from all phonon modes and electron polarization, whereas  $\Delta\varepsilon$  is a contribution of relaxation processes to the static dielectric permittivity. An increase in the dielectric constant with a frequency decrease, leading to a saturation at a constant value,  $\varepsilon_s = \varepsilon_\infty + \Delta\varepsilon$ , was observed in crystalline ionic conductors [18, 19].

It should be mentioned that the frequency dependences of  $\varepsilon'$  in composites with  $x = 0.5$ – $0.9$  can be separated into the following two dispersion regions: (1) from  $10$  to  $2 \times 10^5$  rad/s, and (2) from  $2 \times 10^5$  to  $10^{10}$  rad/s (Fig. 1). These regions are divided by a vertical dash lines in all the following Fig. 3. This

**Table.** Cole-Cole parameters  $\varepsilon_\infty$ ,  $\Delta\varepsilon$ ,  $\alpha$  and  $\tau_0$  of the  $(\text{Ag}_3\text{AsS}_3)_x(\text{As}_2\text{S}_3)_{1-x}$  glasses and composites ( $x = 0.3, 0.4, 0.5, 0.6, 0.8, 0.9$ ) at 300 K.

$x, \text{Ag}_3\text{AsS}_3$		$\varepsilon_\infty$	$\Delta\varepsilon$		$\alpha$		$\tau_0, \text{ms}$	
Disp. reg. $\rightarrow$		1 and 2	1	2	1	2	1	2
(I)	0.3	13.40	41430	–	0.183	–	6.03	–
	0.4	13.90	88090	–	0.185	–	5.84	–
(II)	0.5	15.15	279272	2334	0.222	0.186	2.58	0.02
	0.6	16.18	343028	2605	0.220	0.206	3.33	0.02
(III)	0.8	14.20	225620	571	0.198	0.223	6.91	0.009
	0.9	13.41	261134	613	0.204	0.226	8.66	0.007

Dispersion regions: 1 – from  $10$  to  $2 \times 10^5$  rad/s, 2 – from  $2 \times 10^5$  to  $10^{10}$  rad/s.

corresponds to the maximum with high-frequency asymmetry and a shoulder for composites with  $x = 0.5, 0.6$  as well as two distinct maxima for composites with  $x = 0.8, 0.9$  on the frequency dependences of  $\varepsilon''$  (Fig. 1). This fact supports our results about the phase separation or appearance of crystalline phases. Thus, one has to take two different fitting procedures per graph with respect to the presence of different phases. One should note that for glasses with  $x = 0.3, 0.4$  this process is yet not visible, that is why the X-ray diffraction spectra of the respective glasses reveal no signs of crystalline inclusions [14].

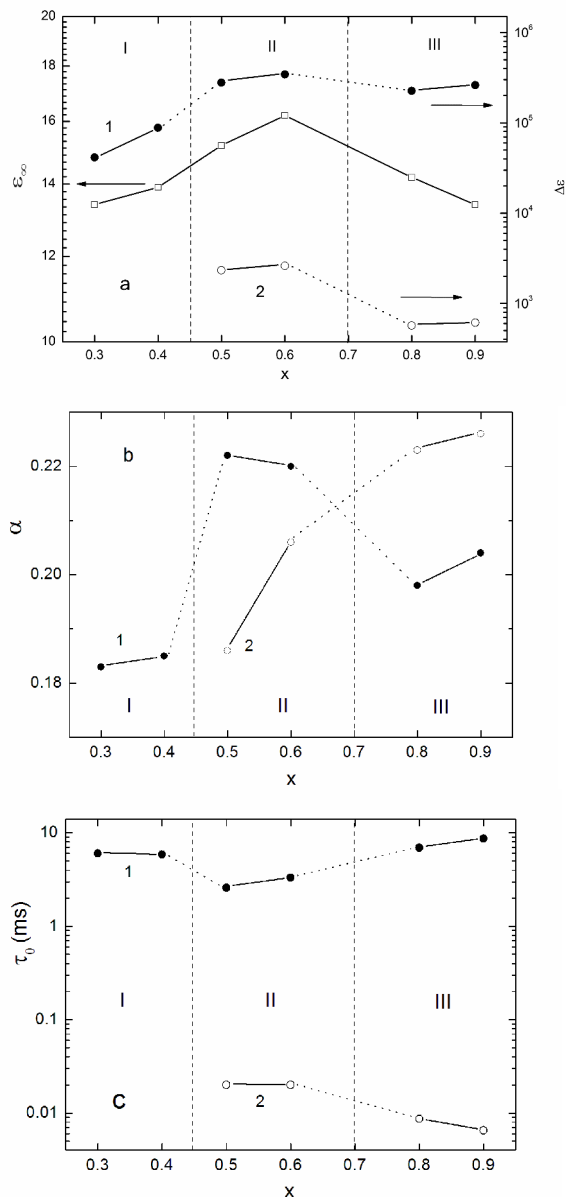


**Fig. 3.** Compositional dependences of the Cole-Cole parameters (a)  $\varepsilon_\infty$  and  $\Delta\varepsilon$ , (b)  $\alpha$  and (c)  $\tau_0$  for  $(Ag_3AsS_3)_x(As_2S_3)_{1-x}$  glasses and composites at 300 K calculated for two dispersion regions: (1) from  $10$  to  $2 \times 10^5$  rad/s, and (2) from  $2 \times 10^5$  to  $10^{10}$  rad/s.

The Cole-Cole parameters determined after performing the fitting procedures are given in Table, while their compositional dependences are highlighted in Fig. 3. Hereby, Fig. 3 shows three compositional states, according to the X-ray studies: the state of amorphous glasses (I) demonstrates one dispersion region and can be fitted by a single Cole-Cole function; the states of composites (II) and (III) demonstrate two dispersion regions, which should be fitted by two different Cole-Cole functions.

The compositional dependences presented in Fig. 3 show that the dielectric strength  $\Delta\varepsilon$  as well as  $\varepsilon_\infty$  nonlinearly varied and reached the highest values in the state (II). An increase of parameter  $\alpha$  with the transition from amorphous to composite structure (from  $x = 0.3, 0.4$  to  $x = 0.5, 0.6$ ) is an expected fact, as far as composite structure with crystalline inclusions is more disordered comparing to glasses, and, hence, have larger distribution of relaxation times. The parameter  $\alpha$  of the second dispersion region demonstrates a permanent enhancement with the  $x$  increase. This substructure, characterized by the second dispersion region, becomes more disordered with the increase of silver content. At the same time, the parameter  $\alpha$  of the first dispersion region displays a decrease after an appearance of proustite  $Ag_3AsS_3$  in the composite with the increase of  $x$  in the  $(Ag_3AsS_3)_x(As_2S_3)_{1-x}$  material. It was shown in [20] that the values of parameter  $\alpha$  like those obtained here for  $(Ag_3AsS_3)_x(As_2S_3)_{1-x}$  glasses and composites are inherent to mixed ionic materials that have one-dimensional ion conducting pathways.

The presence of two different frequency regions in our consideration implies a presence of two different dielectric relaxation processes as well. Therefore, in our results we marked out two modes (which correspond to two used Cole-Cole functions for fitting), the most probable relaxation times of which are given in Fig. 3. Variations of  $\tau_0$  are inversely proportional to the corresponding variations of  $\nu_{max}$  in Fig. 2. The compositional dependence of relaxation times  $\tau_0$  has a minimum in the state (II). Although it is clear that the values of the frequency shoulder at  $x = 0.5, 0.6$  in the frequency region 2 cannot be regarded as fully proper ones. It is worth to remind that the parameter  $\alpha$  also represents the distribution of relaxation times. Further, as we see from Fig. 3, the broadening of the distribution function, i.e. the parameter  $\alpha$  increase, is accompanied, as a rule, by shortening the mean relaxation time  $\tau_0$ .

## 5. Conclusions

Frequency dependences studies of complex dielectric permittivity at 300 K in  $(Ag_3AsS_3)_x(As_2S_3)_{1-x}$  superionic glasses and composites with  $x = 0.3-0.9$  were carried out. A decrease of the real part of dielectric permittivity with frequency by almost 5 orders of magnitude was revealed. One dispersion region for the real part of dielectric permittivity in glasses and two dispersion

regions in composites were observed. They showed single maxima in the dielectric loss function of glasses with  $x = 0.3$  and  $0.4$ , single maxima and peculiarities in the form of high-frequency asymmetry and the shoulder in composites with  $x = 0.5$  and  $0.6$ , as well as two maxima in composites with  $x = 0.8$  and  $0.9$ .

Frequency dependences of the dielectric permittivity within the range from  $10$  to  $3 \times 10^9$  Hz were analyzed in the framework of the Cole-Cole model. Compositional behaviour of the Cole-Cole parameters in  $(\text{Ag}_3\text{AsS}_3)_x(\text{As}_2\text{S}_3)_{1-x}$  ( $x = 0.3-0.9$ ) superionic glasses and composites was studied. Different structural states (glassy, composite) of the investigated materials were considered, and the Cole-Cole fitting procedure involved two dielectric relaxation processes for the composite states. The parameters  $\Delta\varepsilon$ ,  $\varepsilon_\infty$ , and  $\alpha$  reach their highest values in the state (II), whereas  $\tau_0$  gets its minimum. The most essential changes of above mentioned parameters are observed at the transition from glass with  $x = 0.4$  to composite with  $x = 0.5$  as well as from composite with  $x = 0.6$  to composite with  $x = 0.8$ .

#### References

1. K.L. Ngai, J. Habasaki, Y. Hiwatari and C. Leon, A combined molecular dynamics simulation, experimental and coupling model study of the ion dynamics in glassy ionic conductors // *J. Phys.: Condens. Matter*, **15**, p. S1607-S1632 (2003).
2. E. Bychkov, D.L. Price, C.J. Benmore and A.C. Hannon, Ion transport regimes in chalcogenide and chalcogen halide glasses: From the host to the cation-related network connectivity // *Solid State Ionics*, **154-155**, p. 349-359 (2002).
3. E.A. Kazakova and Z.U. Borisova, Electroconductivity of  $(\text{Ag}_3\text{S})_x(\text{As}_2\text{S}_3)_{1-x}$  glass systems // *Fizika Khimii i Stekla*, **6**, p. 424-427 (1980), in Russian.
4. E. Bychkov, A. Bychkov, A. Pradel and M. Ribes, Percolation transition in Ag-doped chalcogenide glasses: Comparison of classical percolation and dynamic structure models // *Solid State Ionics*, **113-115**, p. 691-695 (1998).
5. Yu. Drugov, V. Tsegelnik, A. Bolotov, Yu. Vlasov and E. Bychkov,  $^{110}\text{Ag}$  tracer diffusion study of percolation transition in  $\text{Ag}_2\text{S}-\text{As}_2\text{S}_3$  glasses // *Solid State Ionics*, **136-137**, p. 1091-1096 (2000).
6. E. Bychkov, Superionic and ion-conducting chalcogenide glasses: Transport regimes and structural features // *Solid State Ionics*, **180**, p. 510-516 (2009).
7. M. Krbal, T. Wagner, T. Srba, J. Schwarz, J. Orava, T. Kohoutek, V. Zima, L. Benes, S.O. Kasap and M. Frumar, Properties and structure of  $\text{Ag}_x(\text{As}_{0.33}\text{S}_{0.67})_{1-x}$  bulk glasses // *J. Non-Cryst. Solids*, **353**, p. 1232-1237 (2007).
8. S. Stehlik, J. Kolar, M. Bartos, M. Vlcek, M. Frumar, V. Zima and T. Wagner, Conductivity in Ag-As-S(Se, Te) chalcogenide glasses // *Solid State Ionics*, **181**, p. 1625-1630 (2010).
9. C. Holbrook, P. Chen, D.I. Novita and P. Boolchand, Origin of conductivity threshold in the solid electrolyte glass system  $(\text{Ag}_3\text{S})_x(\text{As}_2\text{S}_3)_{1-x}$  // *IEEE Trans. Nanotechnology*, **6**(5), p. 530-535 (2007).
10. A. Pradel, N. Kuwata and M. Ribes, Ion transport and structure in chalcogenide glasses // *J. Phys.: Condens. Matter*, **15**, p. S1561-S1571 (2003).
11. S. Stehlik, K. Shimakawa, T. Wagner and M. Frumar, Diffusion of Ag ions under random potential barriers in silver-containing chalcogenide glasses // *J. Phys. D: Appl. Phys.* **45**, 205304 (2012).
12. I. Studenyak, Yu. Neimet, C. Cserhati, S. Kókényesi, E. Kazakevicius, T. Salkus, A. Kezionis and A. Orliukas, Structural and electrical investigations of  $(\text{Ag}_3\text{AsS}_3)_x(\text{As}_2\text{S}_3)_{1-x}$  superionic glasses // *Cent. Eur. J. Phys.* **10**, p. 206-209 (2012).
13. I.P. Studenyak, M. Kranjčec, Yu.Yu. Neimet, M.M. Pop, Optical absorption edge in  $(\text{Ag}_3\text{AsS}_3)_x(\text{As}_2\text{S}_3)_{1-x}$  superionic glasses // *Semiconductor Physics, Quantum Electronics & Optoelectronics*, **15**(2), p. 147-151 (2012).
14. I.P. Studenyak, Yu.Yu. Neimet, M. Kranjčec, A.M. Solomon, A.F. Orliukas, A. Kežionis, E. Kazakevičius, and T. Šalkus, Electrical conductivity studies in  $(\text{Ag}_3\text{AsS}_3)_x(\text{As}_2\text{S}_3)_{1-x}$  superionic glasses and composites // *J. Appl. Phys.* **115**, 033702 (2014).
15. A. Kežionis, E. Kazakevičius, T. Šalkus, A.F. Orliukas, Broadband high frequency impedance spectrometer with working temperatures up to 1200 K // *Solid State Ionics*, **188**, p. 110-113 (2011).
16. J.R. Dygas, Dielectric function of ionic conductors studied by impedance spectroscopy // *Solid State Ionics*, **176**, p. 2065-2078 (2005).
17. K.S. Cole and R.H. Cole, Dispersion and absorption in dielectrics I. Alternating current characteristics // *J. Chem. Phys.* **9**, p. 341-351 (1941).
18. K.E.D. Wapenaar and J. Schoonman, Conductivity enhancement in  $\text{Ba}_{1-x}\text{La}_x\text{F}_{2+x}$  solid electrolytes // *Solid State Ionics*, **5**, p. 637-640 (1981).
19. J.B. Bates and J.C. Wang, Dielectric response of ionic conductors // *Solid State Ionics*, **28-30**, p. 115-119 (1988).
20. D.L. Sidebottom, Dimensionality dependence of the conductivity dispersion in ionic materials // *Phys. Rev. Lett.* **83**, p. 983 (1999).